Blending Thermoplastic Polyurethanes and Poly(ethylene oxide) for Composite Electrolytes Via a Mixture Design Approach

TEN-CHIN WEN, WEI-CHIH CHEN

Department of Chemical Engineering, National Cheng Kung University, Tainan, 701, Taiwan

Received 23 June 1999; accepted 16 November 1999

ABSTRACT: With the aim of obtaining proper composite electrolytes, a systematic modeling analysis for the percentage increase in weight due to swelling with respect to swollen weight, S_w, and the room temperature conductivity (σ_{25}) of the composite films of polyethylene glycol based thermoplastic polyurethane/polytetramethylene glycol based thermoplastic polyurethane/polyethylene oxide [denoted as TPU(PEG)/TPU(PTMG)/PEO] was performed. Using a mixture design approach, empirical models are fitted and plotted as contour diagrams which facilitate revealing the synergistic/antagonistic effects among the mixed polymers. The contour plot results show that both the maximum S_w (64.9%) and the maximum σ_{25} (72.2×10^{-5} S cm^{-1}) appear at point X_3 (PEO 85%, TPU(PEG) 15%). The results are reasonably explained from the interactions among polymers on the basis of their molecular structures. The thermal analysis of the composite films is performed to demonstrate the speculations about the interactions among the mixed polymers by using differential scanning calorimeter. The crystallization of PEO spherulites at different compositions was examined by using a polarizing microscope. © 2000 John Wiley & Sons, Inc. J Appl Polym Sci 77: 680–692, 2000

Key words: polyurethane; composite electrolyte; conductivity; polymer blending; mixture design

INTRODUCTION

Many studies of physical mixtures of polymer/oligomer or polymer/polymer pairs have been reported in the literature in the past few years. In many cases, when the components have proton doner and proton acceptor capabilities, hydrogen bonding is sufficient to obtain miscible blends.[1–3] However, there are few papers concerning polyurethanes and poly(ethylene oxide) (PEO) blends which were subsequently used as solid polymer electrolytes.

Solid polymer electrolytes have attracted much attention for their ability to produce safe, flexible, and thin plastic batteries. The first system of solid polymer electrolytes, PEO-LiX (X = ClO_4^-, $CF_3SO_3^-$), was discovered by Wright[4] and the application to lithium batteries was pointed out by Armand et al.[5] In the PEO-LiX system, the PEO provides the ethylene oxide structure to stabilize the lithium ion and to uncoil the polymer chain for migration of ions. However, the PEO-LiX system shows poor conductivity at room temperature because the ions possess low mobility in PEO film because of its high crystallinity. To increase the conductivity, polar solvents, such as propylene carbonate (PC) or ethylene carbonate, were added

Correspondence to: T.-C. Wen (tcwen@mail.ncku.edu.tw).

Contract grant sponsor: National Science Council of the Republic of China; contract grant number: NSC 89-2214-E-006-012.

Journal of Applied Polymer Science, Vol. 77, 680–692 (2000)

to the polymer matrix to form gel electrolytes. In our laboratory, the same result in waterborne polyurethane (WPU) has been reported.[6] Unfortunately, the addition of solvents always weakens the polymer strength for insulation between anode and cathode.

To improve both conductivity and strength, dual-phase polymer electrolytes by polyblends nitrobutyronitrile and styrene butadiene rubber were proposed,[7–12] which consist of a polar polymer to take up lithium salt solution and a nonpolar polymer to provide the strength. Results from this laboratory on the WPU(PTMG)/PEO based electrolyte system[13] proved to possess the dual phase characteristics of polymer composites in which PEO absorbs $LiClO_4$-PC to form the ion conducting phase whereas WPU(PTMG) only provides the strength. WPU(PTMG)/PEO electrolytes possess a very good room temperature conductivity of ca. 10^{-2} S cm^{-1} with a specific polymer composition.[13] Meanwhile, our previous articles[14,15] revealed that conductivity values of WPU(PEG) based electrolyte increase with increasing $LiCF_3SO_3$-PC content. The electrolyte containing 70% $LiCF_3SO_3$-PC was found to possess good conductivity of $\approx 10^{-3}$ S cm^{-1} but was associated with poor strength for insulating the anode from the cathode at high temperature (≈80°C).[15] This was ascribed to the presence of the soft segment, —(C—C—O)—, which can absorb electrolyte easily.

However, there are some disadvantages with WPU. The strength, complex molecular structure, the ease for decomposition easily at high temperature are the few limitations.[15] The present study aims to use thermoplastic polyurethanes to overcome the difficulties with WPU. From the viewpoint of molecular structure, TPU(PEG) possesses the same hard and soft segments as that of TPU(PTMG) and PEO, respectively. Accordingly, it might be used as an interfacial promoter for the composites to improve the miscibility. Therefore, a promising property can be expected by mixing TPU(PEG), TPU(PTMG), and PEO to improve the properties of the electrolyte.

Our laboratory has successfully proposed a mixture design approach to analyze some important properties of a ternary system.[16–18] This method assumes that the properties of the composite electrolyte are a function of the composition of the components [TPU(PEG), TPU(PTMG), PEO] involved. This relationship can be expressed as:

$$\eta = f(x_1, x_2, x_3)$$

where the variable x_i represents the weight proportions of TPU(PEG), TPU(PTMG), and PEO, respectively, in the composite film. In this study, a design matrix with 16 experiments and a forward stepwise regression procedure were used to achieve a statistically significant regression equation. The regression models were then plotted as the contour diagrams of room temperature conductivity (σ_{25}), S_w and the conductivity per unit percentage swelling (σ_s) against composition, which facilitated straightforward interpretations of the conductivities of binary and ternary systems.

Because TPU(PTMG) and PEO are not suitable to be used as the matrix of polymer electrolyte alone, 15% TPU(PEG) was set as the lower limit of the composition for all composite films. Thus, the design matrix of the pseudo-components (x_1, x_2, and x_3) as well as the real compositions (y_1, y_2, and y_3) are listed in Table I, in which the real compositions are calculated from the pseudo-components (x_1, x_2, and x_3) with the equations shown as follows:

$$y_1 = 0.85\ x_1 + 0.15;\ y_2 = 0.85\ x_2;\ y_3 = 0.85\ x_3;$$

where the subscripts 1, 2, and 3 represent the component TPU(PEG), TPU(PTMG), and PEO, respectively. The details can be seen in our previous article.[17]

EXPERIMENTAL

Materials

The raw materials used in this study are listed in Table II. Poly(ethylene glycol) (PEG) and poly(tetramethylene glycol) (PTMG) were dried and degassed in a vacuum oven under 85°C for 1 day. All other chemicals were used without further treatment.

Procedure

Synthesis of Thermoplastic Polyurethane (TPU)

An outline of the process used in this study for preparation of PEG and PTMG based TPU dispersions [noted as TPU(PEG) and TPU(PTMG), respectively] is shown in Scheme 1. The TPU(PEG) and TPU(PTMG) prepolymers were synthesized by a one-step addition reaction. A 2000-mL four-necked round-bottom flask equipped with an

Table I Design Matrix and Experimental Results of TPU(PEG)-TPU(PTMG)-PEO Composite Electrolytes

Sample	Pseudocomponent			Real Composition			S_w (wt %)	σ_{25} ($\times 10^{-5}$ S cm^{-1})	σ_s ($\times 10^{-7}$ S cm^{-1})
	x_1	x_2	x_3	y_1	y_2	y_3			
1	1	0	0	1.00	0.00	0.00	57.1	35.00	61.35
2	0	1	0	0.15	0.85	0.00	36.4	0.36	0.98
3	0	0	1	0.15	0.00	0.85	64.9	72.20	111.23
4	1/3	1/3	1/3	0.43	0.28	0.28	51.7	34.50	66.8
5	1/2	1/2	0	0.58	0.43	0.00	42.6	14.30	33.6
6	0	1/2	1/2	0.15	0.43	0.43	55.6	75.10	135.02
7	1/2	0	1/2	0.58	0.00	0.43	59.4	51.30	86.38
8	3/4	1/4	0	0.79	0.21	0.00	43.5	17.90	41.23
9	1/4	3/4	0	0.36	0.64	0.00	41.7	1.40	3.35
10	0	3/4	1/4	0.15	0.64	0.21	50.0	4.83	1.57
11	0	1/4	3/4	0.15	0.21	0.64	62.9	60.50	86.2
12	1/4	0	3/4	0.36	0.00	0.64	63.0	55.20	87.62
13	3/4	0	1/4	0.79	0.00	0.21	58.2	43.20	74.23
14	2/3	1/6	1/6	0.72	0.14	0.14	55.6	27.50	49.54
15	1/6	2/3	1/6	0.29	0.57	0.14	30.8	0.77	1.57
16	1/6	1/6	2/3	0.29	0.14	0.57	64.7	53.40	82.48

Note: The subscripts 1, 2, and 3 represent the components TPU(PEG), TPU(PTMG), and PEO, respectively.

anchor-propeller stirrer, a nitrogen inlet and outlet, and a thermocouple was connected to the temperature controller.

PEG or PTMG (100 g, 0.1 mol) and methylene bis (*p*-cyclohexyl isocyanate) (H_{12}MDI) (81.33 g, 0.31 mol) were simultaneously added to the reactor which was charged under a nitrogen gas atmosphere, to form a prepolymer of TPU where the ratio of NCO/OH is 3. The temperature was kept at 50°C initially. After proper mixing (100 rpm), two drops of di-*n*-butyltin (IV) dilaurate (DBTDL, catalyst) were added into the batch to catalyze the reaction and then the temperature was raised to 85°C. After 6 h of reaction, 700 g of dimethylformamide (DMF) was added. Then, the chain extender, ethylenediamine (12.6 g, 0.21 mol) which was previously diluted to a 10% solution in DMF, was added slowly to convert the prepolymers into polymers. The viscosity was found to increase in this step. After 1 h reaction, several drops of methyl alcohol (MeOH) were added to terminate the reaction.

Molecular Weight

The average molecular weights, $\bar{M}_n$ and $\bar{M}_w$, were determined by use of a Shimadzu GPC fitted with a Shimadzu HPLC pump and a differential refractometer. A Jordi gel DVB mixed-bed 250 × 10 mm column was used for the analysis. DMF was used as the continuous phase and was pumped through the column at a flow rate of 2.0 mL/min. This system was calibrated against 10 polystyrene standards. The measured molecular weight

Table II Raw Materials for TPU(PEG)/TPU(PTMG) Polymerization

Designation	Chemical Identification	Suppliers
PEG	Polyethylene glycol, M_w = 1000	Showa Chemical, Inc. (Tokyo, Japan)
PTMG	Polytetramethylene glycol, M_w = 1000	Showa Chemical, Inc. (Tokyo, Japan)
H_{12}MDI	Methylene bis (*p*-cyclohexyl isocyanate)	Aldrich Chemical, Inc. (Milwaukee, WI)
DMF	Dimethylformamide	Tedia Company, Inc. (Fairfield, Ohio)
EDA	Ethylenediamine	Merck Chemical, Inc. (Darmstadt, Germany)
MeOH	Methyl Alcohol	Tedia Company, Inc. (Fairfield, Ohio)

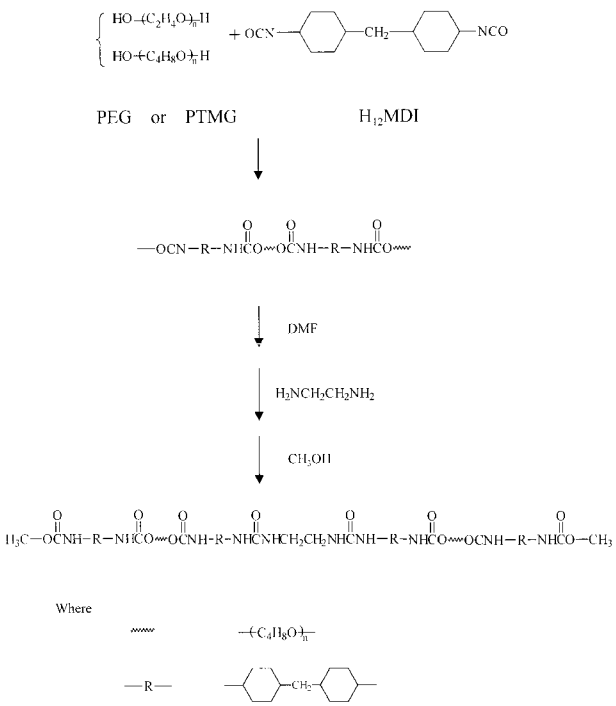

Scheme 1 Polymerization of thermoplastic polyurethane.

and molecular weight distribution of the synthesized TPUs are given in Table III.

Tensile Strength

The mechanical properties of the cast films were determined using an EEKON Instron tensile tester, according to ASTM D-412 specifications, at a cross head speed of 500 mm/min with a full scale load cell at 25 kg. The averages of at least five measurements are reported herein.

Preparation of the Composite Electrolytes

The prepared TPU(PEG) and TPU(PTMG) blends were mixed with the DMF solution of polyethylene oxide (PEO, $\bar{M}_w$. 4×10^5; Aldrich Chemical, Milwaukee, WI) in the desired ratio according to the design matrix in Table I to form uniform solutions. These solutions were then heated and stirred under 70°C for 4 h and poured into a glass disk to cast film. The films were then dried under vacuum at 50°C for 7 days and stored in an argon filled dry box (Vacuum Atmosphere Company, Hawthorne, CA, USA). The thickness of the films was controlled to be between 100≈150 μm.

Lithium perchlorate, $LiClO_4$ (anhydrous; Anderson Phys. Lab.) was dissolved in propylene carbonate (PC) (anhydrous, 99.7%; Aldrich Chemical) to form 1*M* $LiClO_4$-PC solutions in dry box.

Swelling Studies

The composite electrolytes were prepared by dipping dried TPU(PEG)/TPU(PTMG)/PEO composite films into 1*M* $LiClO_4$-PC solution for 10 min at room temperature in a dry box. S_w of various composite films in $LiClO_4$-PC solution was measured to investigate its dependence on composition and the effect on conductivity. The percentage increase in weight due to swelling with respect to swollen weight, S_w, was determined by using:

$$S_w = 100(W - W_0)/W$$

W_0 is the weight of the dried film and W is the weight of the film at 10 min swelling.

Conductivity Measurement

The conductivity of the composite electrolyte was measured via impedance analysis with an electrochemical cell consisting of the electrolyte film sandwiched between two blocks of stainless steel, sealed with an O-ring in a tube which was covered with a jacket for heating/cooling water circulation. The temperature of the cell was controlled using a water thermostat (HAAKE D8 & G) and calibrated using a Pt resistance thermometer. The impedance analysis was performed by using a CMS300 EIS system (Gamry Instruments, Inc., USA) with SR810 DSP lock-in amplifier (Standford Research Systems, Inc., USA) under an oscillation potential of 10 mV from 100 kHz to 1 kHz. The conductivity was calculated by:

$$\sigma = \frac{1}{R_b} \times \frac{l}{A}$$

where R_b is the bulk resistance from AC impedance, ℓ is the film thickness, and A is surface area of electrode.

Table III Molecular Weight and Its Distribution of the Synthesized TPUs

TPU Code	$M_n \times 10^{-4}$	$M_w \times 10^{-4}$	M_w/M_n
TPU(PEG)	8.9	24.9	2.79
TPU(PTMG)	16.3	28.4	1.74

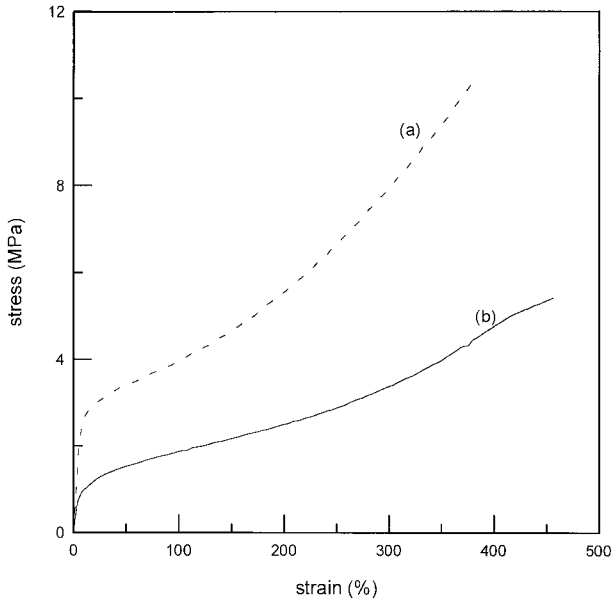

Figure 1 Stress-stain curves of TPU cast films; (a) TPU(PTMG), (b) TPU(PEG).

Thermal Analysis

Thermal analysis of the composite films was performed on a DuPont DSCr 2010 differential scanning calorimeter with a heating rate of 10°C/min and over the temperature range −100 to 100°C. Samples taken from the composite films were sealed in aluminum capsules and transferred out of the dry box to perform thermal analysis.

Morphology

A Nikon Optiphot2-POL polarizing microscope (PM) equipped with a Nikon NFX-35 camera was used to investigate the morphologies of the composite films. The samples were prepared by dropping a prepared polymer solution onto a microscope cover slip and drying under atmospheric conditions and then under vacuum for several days.

RESULTS AND DISCUSSION

Mechanical Properties of TPU

Stress-strain curves of TPU cast films are illustrated in Figure 1, exhibiting the similar stress-strain behavior with a typical form of flexible plastic polymers.[19] For the convenience of discussion, the stress-strain curve was divided into two regions. In the first region, ie., the region of elastic deformation, stress increases linearly with strain and then, beyond the yield point to the plastic deformation, the stress starts to level off. The initial elastic deformation prior to the yield point arise due to the result of bending and stretching of the covalent bonds in the polymer backbone along with recoverable uncoiling of polymeric chains. After this region, the irreversible slippage of polymeric chains can cause the plastic deformation. The differences in the repeat units of the selected polymers/polymeric blends and intermolecular forces operative in these structures are the main reasons for observed results related to the mechanical properties.

The data of mechanical properties are listed in Table IV. A comparison of the mechanical properties between the TPU(PEG) and TPU(PTMG) showed that, in general, TPU(PTMG) had a higher modulus and stress than those of TPU-(PEG), except for the yield strain and ultimate elongation. For the modulus of resilience, which is the capacity of a material to absorb energy when it is deformed elastically in the elastic region and then, upon unloading, to have this energy recovered. The modulus of resilience (U_r) is defined as eq. (1):

$$U_r = \int_0^{\varepsilon_y} s \, d \, \varepsilon \tag{1}$$

in which s is the stress and ϵ_y is the strain at yielding.

Another mechanical term, toughness, is a measure of the ability of a material to absorb energy up to fracture. Furthermore, fracture toughness is a property indicative of a material's resistance to fracture when a crack is present. The actual value of toughness is calculated by integrating

Table IV Mechanical Properties of TPU(PEG) and TPU(PTMG)

Specification	TPU(PEG)	TPU(PTMG)
Young's modulus (MPa)	21.9	52.1
Yield strength (MPa)	0.63	1.36
Yield strain (%)	3.25	2.80
Tensile strength (MPa)	5.41	10.4
Ultimate elongation (%)	456	380
Modulus of resilience (MPa)	9.75×10^{-3}	1.90×10^{-2}
Toughness (MPa)	13.4	21.9

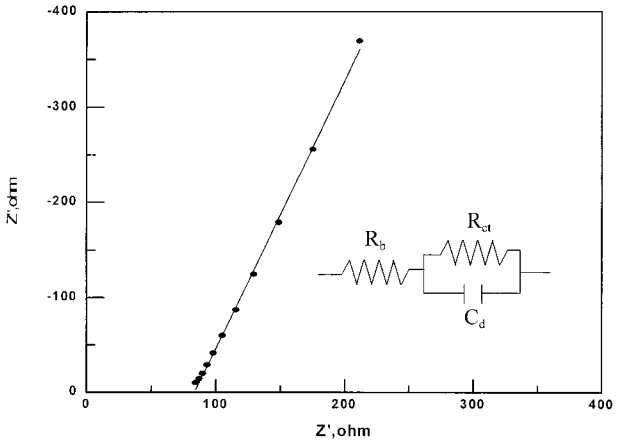

Figure 2 Nyquist plot of SS/CE(sample 1)/SS at 25°C. The CE film is composed of 42.9% TPU(PEG), and 57.1% 1*M* $LiClO_4$/PC. The CE film is 110 μm in thickness and 0.785 cm^2 in area. Impedance frequency range: 100 kHz to 1 kHz.

the area under the stress-strain curve up to the point of fracture. The higher values of most mechanical properties for TPU(PTMG) than those for TPU(PEG) is probably due to the higher molecular weight (see Table III) for TPU(PTMG) and its molecular structure. Polymers with high molecular weight possess strong intermolecular forces due to the longer chains and consequent interactions. For polyurethanes, high magnitude of mechanical properties results from strong intermolecular forces between the rigid and flexible segments.

AC Impedance

To demonstrate the reliability of σ data, the experiments for obtaining σ are discussed first. The AC (alternating current) impedance of all samples in Table I sandwiched between stainless steel (SS) electrodes was performed to obtain the Nyquist plots with an equivalent circuit as shown in Figure 2 for sample 1. A straight line is presented in a high-frequency region and simulated by an equivalent circuit of charge transfer resistance (R_{ct}) and double-layer capacitance (C_d) parallel to each other and bulk resistance (R_b) in series. The mathematics for impedance (Z) of this equivalent circuit can be expressed as:

$$Z = \left(R_b + \frac{R_{ct}}{1 + (R_{ct}\omega C_d)^2}\right) - \left(\frac{R_{ct}^2\omega C_d}{1 + (R_{ct}\omega C_d)^2}\right)j \quad (2)$$

where ω is the angular frequency and j represents the imaginary part of Z. From the denominator, $1 + (R_{ct}\omega C_d)$ in eq. (2), the order of magnitude of this dimensionless group, $R_{ct}\omega C_d$, in comparison with unity is very important to the analysis of a physical system. According to an engineering viewpoint, there are two extreme cases: (i) when $R_{ct}\omega C_d \gg 1$, then $Z \rightarrow R_b$, while (ii) when $R_{ct}\omega C_d \ll 1$, then $Z \rightarrow R_b + R_{ct}$.

In this study, since the charge-transfer reaction is extremely difficult to occur under a small oscillation potential due to SS electrodes, $R_{ct}C_d$ is too large to have the arc for locating $R_b + R_{ct}$. The straight line represents the response of a C_d in parallel with a large R_{ct}. Thus, with increasing ω, the straight line intercepts the real axis to locate R_b. For presenting conductivity (σ) value, R_b obtained from AC impedance is transferred by using the relationship $\sigma = (1/R_b)(\ell/A)$, where ℓ and A represent the film thickness and surface area of an electrode, respectively.

Arrhenius Plots of Conductivity

After data manipulation, log(σ) vs 1000/T(K) can be plotted in Figure 3, showing three straight lines for samples 1≈3 films in Table I. Note that these three lines are approximately parallel to one another, indicating that the conductivity of TPU electrolytes obeys the Arrhenius law due to the similar conducting environment. This implies that the conductive environment of Li^+ in these TPU electrolytes is

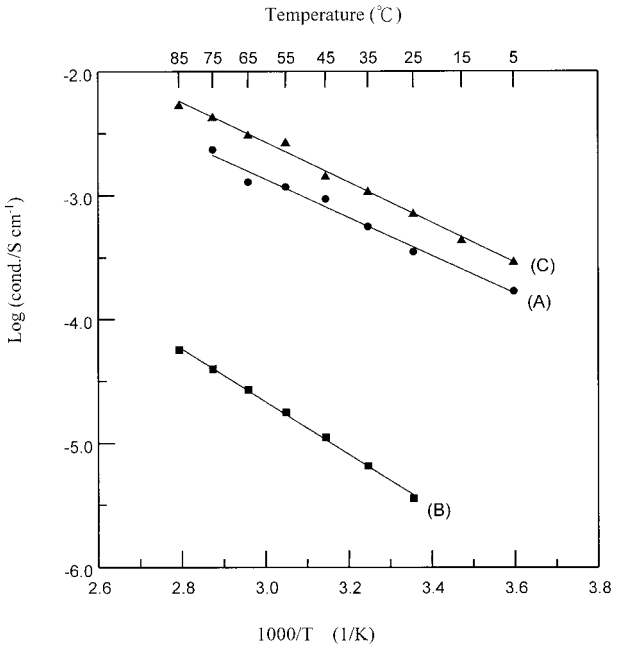

Figure 3 Arrhenius plots of conductivity for three different electrolytes. (A) sample 1; (B) sample 2; and (C) sample 3.

Table V Analysis of Variance for the Fit of S_w for the Composite Films Measured at Room Temperature

Source	Degrees of Freedom	Sum of Squares	Mean Square	F Value
Model	4	45331.76	11332.94	559.96
Error	12	242.87	20.24	
Total	16	45574.63		

$R^2 = 0.9947$; $R^2_{adj} = 0.9929$.

liquid-like and remains unchanged in the investigated temperature region. From Figure 3, it is clear that the conductivity increases evidently with increasing temperature. The activation energy (E_c) of conductivity for various films can be calculated from the Arrhenius equation:

$$\sigma = \sigma_0 \exp(-E_c/RT) \tag{3}$$

where T is temperature on the Kelvin scale and σ_0 is a proportional constant. E_c values of sample 1, sample 2, and sample 3 are 29.3 kJ/mol, 40.6 kJ/mol, and 30.8 kJ/mol, respectively. Among these three samples, sample 2 possesses the largest activation energy, the two others are almost the same. High activation energy implies that σ of the electrolyte is very sensitive to temperature. The reasons why σ follows the order as sample 3 > sample 1 > sample 2, will be explained below.

Regression Analysis of S_w and σ_{25}

The conductivity (σ) of the composite electrolyte is considered to be related to S_w of liquid electrolyte which is responsible for the ionic conduction. In this study, the swelling time is controlled at 10 min for all composite electrolytes to investigate S_w and its effect on σ. The data of S_w and σ_{25} (the subscript indicates the temperature in degree C) are listed together with the design matrix in Table I. Coefficients of the regression equations for σ_{25} and S_w approximation models were calculated from the experimental values in Table I with the aid of the appropriate formula[20] and the following equations were generated:

$$S_w = \underset{(2.66)}{53.70\, x_1} + \underset{(2.79)}{37.10\, x_2} + \underset{(2.66)}{69.65\, x_3} - \underset{(280.37)}{571.55\, x_1 x_2^2 x_3} \tag{4}$$

$$\sigma_{25} = \underset{(6.42)}{28.57 x_1} + \underset{(8.35)}{66.50 x_3)} + \underset{(34.30)}{54.44 x_2 x_3} - \underset{(77.06)}{133.82 x_2 x_3 (x_2 - x_3)} \tag{5}$$

where x_1, x_2, and x_3 represent the pseudo-components of TPU(PEG), TPU(PTMG), and PEO, respectively, in the composite films. The numbers in parentheses below the coefficients are their standard errors based on error variance estimates (s^2 = mean square of error = 20.24 for S_w and 124.72 for σ_{25}).

The analysis of variances of S_w and σ_{25} are summarized in Tables V and VI, respectively. The test statistics, F and R^2_{adj}, are defined as F = MSR/MSE and $R^2_{adj} = 1 - [SSE/(N - P)/SST/(N - 1)]$, where MSR is the mean square of regression obtained by dividing the sum of squares of regression with the degree of freedom. MSE represents mean square error from the analysis of variance. If the calculated F value is greater than the table $F(P - 1, \nu, 1 - \alpha)$ value, a "statistically significant" regression model is obtained, where ν is the degree of freedom of error and P is the number of parameters. $F(P - 1, \nu, 1 - \alpha)$ is the F value at the α probability level. R^2_{adj} is the adjusted correlation coefficient (R^2), with a value close to 1 meaning a perfect fit to the experimental data (0.9929 for S_w and 0.9303 for σ_{25}).

From the statistical point of view, the magnitude of the regression equation coefficients compared with their estimated standard errors are used as the basis for judging statistical significance and illustrating the relative effects (synergistic/antagonistic) of the composition on S_w and σ_{25}. The main effects of TPU(PEG) on S_w and σ_{25} are indicated by the coefficient associated with the x_1 terms, which are 53.70 and 28.57, respectively. In comparison to TPU(PEG), the coefficients for x_2 terms for [TPU(PTMG)] are 37.10

Table VI Analysis of Variance for the Fit of Conductivity for Polymer Films Measured at 25°C

Source	Degrees of Freedom	Sum of Squares	Mean Square	F Value
Model	4	27135.42	6783.86	54.393
Error	12	1496.62	124.72	
Total	16	28632.04		

$R^2 = 0.9477$; $R^2_{adj} = 0.9303$.

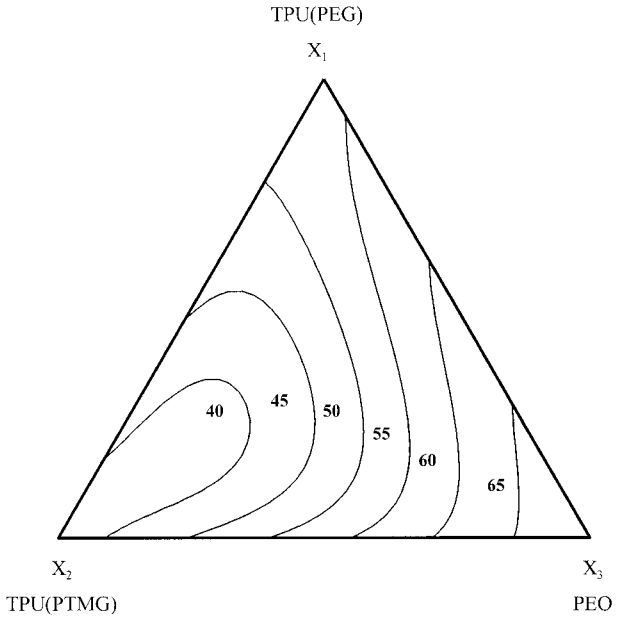

Figure 4 A contour plot of swollen weight in weight percent against TPU(PEG)-TPU(PTMG)-PEO based electrolytes at 25°C.

and 0 for S_w and σ_{25}, respectively, implying that TPU(PTMG) employs no contribution on σ_{25}. Similarly, the main effects of PEO on S_w and σ_{25} are indicated also by the magnitude of the coefficients associated with x_3 terms, which are 69.65 and 66.50, respectively. The terms of x_2x_3 and higher order terms indicate the effects of the interactions between various polymers on S_w and σ_{25}. To facilitate a straightforward examination of the dependence of S_w and σ_{25} on the polymer compositional diagram, the contour lines of S_w and σ_{25} were plotted by using eqs. (4) and (5) in Figures 4 and 5, respectively.

An examination of S_w contour lines reveals two features: 1. the minimum S_w occurs at point X_2 [85% TPU(PTMG), 15% TPU(PEG)] and the maximum S_w occurs at point X_3 [85% PEO, 15% TPU(PEG)]; 2. along lines X_2-X_3 [TPU(PTMG)-PEO] or X_2-X_1 [TPU(PTMG)-TPU(PEG)], S_w is increased by increasing PEO or TPU(PEG) composition; as for X_1-X_3 [TPU(PEG)-PEO], S_w increases slightly with increasing PEO.

The above results can be reasonably explained from the viewpoint of the molecular structures of TPU(PTMG), TPU(PEG), and PEO. Definitely, PEO can absorb $LiClO_4$-PC easily due to the high polarity of its repeat unit, —(C—C—O)—. Because TPU(PEG) possesses the same repeat unit, —(C—C—O)—, for its soft segment, it is surely considered to have similar swelling capability as PEO. However, it also possesses the urethane group for the hard segment which provides hydrogen bonding to increase the film strength and simultaneously hinder the absorption of $LiClO_4$-PC electrolyte, being ranked as the second for the electrolyte swelling and the strength. As for TPU(PTMG), due to the low polarity of the soft segment, —(C—C—C—C—O)—, and the hydrogen bonding from the urethane group, it possesses the best strength and the worst swelling capability for $LiClO_4$-PC electrolyte, being reasonably conceivable. Accordingly, increasing PEO content in TPU(PTMG)-PEO and/or TPU(PEG)-PEO or TPU(PEG) in TPU(PEG)-TPU(PTMG) surely increases S_w.

An examination of the contour lines of σ_{25} (Fig. 5) reveals some similar features as S_w: 1. the minimum σ_{25} occurs at point X_2 [85% TPU(PTMG), 15% TPU(PEG)]; 2. σ_{25} is increased by increasing PEO/TPU(PEG) composition along lines X_2-X_3 [TPU(PTMG)-PEO] or X_2-X_1 [TPU(PTMG)-TPU(PEG)]; 3. for line X_1-X_3 [TPU(PEG)-PEO], σ_{25} increases slightly with increasing PEO and then reaches an extreme value in this binary system. A comparison between the maximum S_w (64.9%) and the maximum σ_{25} (72.2×10^{-5} S cm^{-1}) reveals that these two extreme values both occur at point X_3, evidence that σ_{25} is a function of S_w.

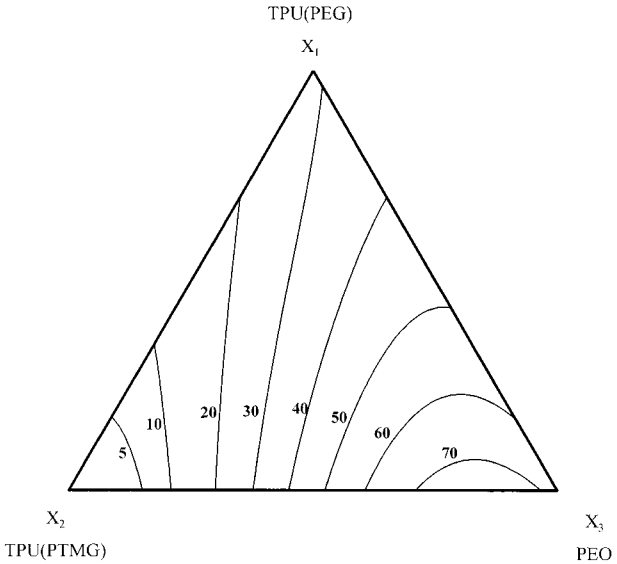

Figure 5 A contour plot of conductivity in ($\times 10^{-5}$)S cm^{-1} against TPU(PEG)-TPU(PTMG)-PEO based electrolytes at 25°C.

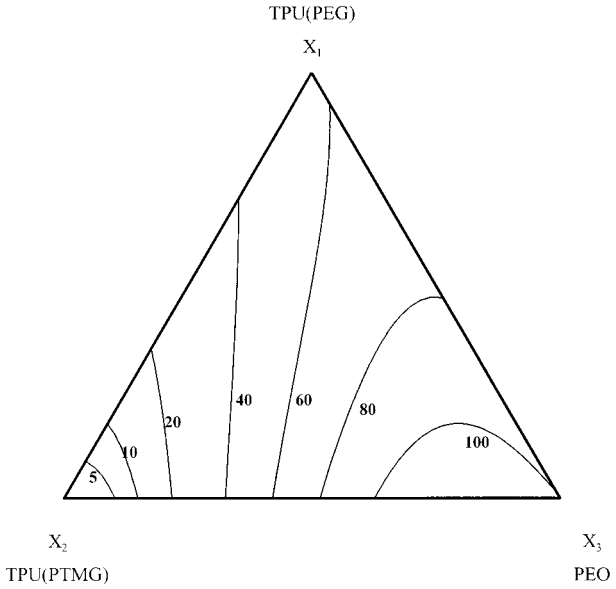

Figure 6 A contour plot of σ_s in $(\times 10^{-7})S$ cm^{-1} against TPU(PEG)-TPU(PTMG)-PEO based electrolytes at 25°C.

As mentioned above, TPU(PEG) possesses the same soft segments as PEO and hard segments as TPU(PTMG). Accordingly, TPU(PEG) might be partially miscible with both PEO and TPU(PTMG). The increased TPU(PEG) content in TPU(PEG)-TPU(PTMG) binary, leads to the increase in both S_w and σ_{25} along lines X_2-X_1. Similarly, the increased PEO content in TPU(PEG)-PEO and TPU(PTMG)-PEO binaries, leads to the increase in both S_w and σ_{25} along lines X_1-X_3 and X_2-X_3, respectively. On the line X_2-X_3, σ_{25} increases significantly with increasing PEO (i.e., increasing S_w) due to the formation of continuous PEO phase.

In the above discussion, since only the effect of S_w on σ_{25} was considered, another index, polymer molecular structure was examined by the specific conductivity (σ_s) which was obtained by dividing σ_{25} with S_w. These values imply the conductivity of three different polymer films that absorb the same weight percentage of $LiClO_4$-PC. If molecular structure has no influence on the conductivity, the values of σ_s in all compositions are the same; however, σ_s is not a constant value. This result implies that σ depends not only on S_w but also on the polymer molecular structure. Equation (6) is the regression equation of σ_s and Figure 6 is the counter plot by using eq. (6). The values of σ_s are listed in Table I. The analysis of variances for σ_s are summarized in Table VII. The test statistics, R^2 and R^2_{adj} are 0.9920 and 0.8960, respectively.

$$\sigma_2 = \underset{(13.02)}{56.82x_1} + \underset{(16.94)}{100.54x_3} + \underset{(69.61)}{106.52x_2x_3} - \underset{(156.38)}{207.28x_2x_3(x_2 - x_3)} \quad (6)$$

From this equation, it is obvious that σ_s is influenced by terms x_1 and x_3, as well as interaction term x_2x_3.

An examination of contour lines of σ_s (Fig. 6) reveals almost the same features as σ_{25}: 1. the minimum σ occurs at point X_2 [85% TPU(PTMG), 15% TPU(PEG)]; 2. σ is increased by increasing PEO and/or TPU(PEG) composition along the X_2-X_3 [TPU(PTMG)-PEO] or X_2-X_1 [TPU(PTMG)-TPU(PEG)] lines; 3. for X_1-X_3 [TPU(PEG)-PEO], σ increases slightly with increasing PEO and then reaches an extreme value in this binary system. A comparison between the maximum σ_{25} (72.2×10^{-5} S cm^{-1}) and the maximum σ_s (113.23×10^{-7} S cm^{-1}) reveals that both the extreme values occur at point X_3.

The above results can be reasonably explained from the molecular structures of TPU(PTMG), TPU(PEG), and PEO. $LiClO_4$, due to the high polar repeat unit of PEO, —(C—C—O)—, would be dissociated to Li^+ and ClO_4^- easily, rendering the high conductivity. Because TPU(PEG) possesses the same repeat unit, —(C—C—O)—, for its soft segment, it is surely considered to have the similar conductivity as PEO. However, it also possesses urethane group for the hard segment, which provides hydrogen bonding to stabilize Li^+, so Li^+ cannot move easily. Therefore, TPU(PEG) possesses lower conductivity than PEO. As for TPU(PTMG), due to the low polarity of the soft segment, —(C—C—C—C—O)—, and the hydrogen bonding from the urethane group, it is difficult to dissociate $LiClO_4$ and stabilize Li^+. For these reasons, TPU(PTMG) has the minimum σ,

Table VII Analysis of Variance for the Fit of σ_s for Polymer Films Measured at 25°C

Source	Degrees of Freedom	Sum of Squares	Mean Square	F Value
Model	4	72848.01	18212.00	35.461
Error	12	6163.01	513.58	
Total	16	79011.03		

$R^2 = 0.9220$; $R^2_{adj} = 0.8960$.

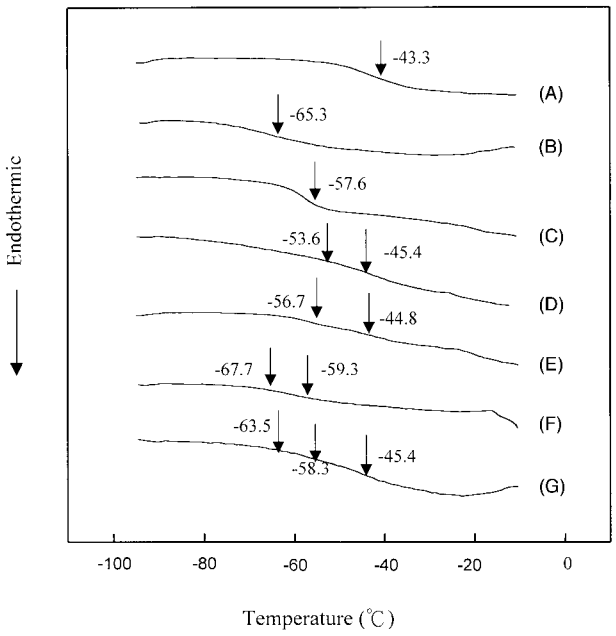

Figure 7 DSC thermograms of TPU blends. (A) TPU-(PEG), (B) TPU(PTMG), (C) PEO, (D) TPU(PEG)/PEO 50/50, (E) TPU(PEG)/TPU(PTMG) 50/50, (F) TPU-(PTMG)/PEO 50/50, and (G) TPU(PEG)/TPU(PTMG)/PEO 33/33/33.

under the same intake of $LiClO_4$-PC. Accordingly, the increase in PEO content in TPU(PTMG)-PEO and/or TPU(PEG)-PEO or TPU(PEG) in TPU-(PEG)-TPU(PTMG) surely increases σ.

Thermal Analysis

Basically, the above discussion is based on the hypothesis that TPU(PTMG)-PEO is immiscible whereas TPU(PEG)-TPU(PTMG) and TPU(PEG)-PEO are partially miscible. To investigate the degree of miscibility of TPU and TPU/PEO blends, differential scanning calorimeter analysis was performed. Figure 7 shows the glass transition temperature (T_g) of various polymers and in each thermogram, the T_gs which are shown by arrows. The temperature region (ΔT_g) for pure component (curves A $\approx$ C) is relatively narrow, but is broad for the blends (curves D $\approx$ G), as can be seen from the figure. On curves D $\approx$ G with broad ΔT_g, there are two or three different slopes, which implies two or three T_gs in each composite. A comparison among curves A, C, and D reveals that the T_g of PEO shifts to a higher temperature, as TPU(PEG) blends with PEO, and the T_gs of TPU(PEG) in curves A and D are almost the same. A comparison among curves A, B, and E gives similar results. These results validate that TPU(PEG)/PEO and TPU(PEG)/TPU(PTMG) are partially miscible and the degree of miscibility in TPU(PEG)/TPU(PTMG) is higher than in TPU-(PEG)/PEO. However, the range of two T_gs on curve F are very similar with the T_gs of TPU-(PTMG) and PEO on curves B and C, respectively, which implies that TPU(PTMG) and PEO are not miscible. In the ternary blend (curve G), the three T_gs are little closer than their original values. Accordingly, TPU(PEG) is an interfacial promoter for the composites to improve the miscibility.

T_m and crystallinity might also provide some index for the miscibility of these composites. Thermograms of pure PEO and TPU/PEO blends are shown in Figure 8. Because TPU-(PEG) and TPU(PTMG) possess an amorphous structure, their DSC traces are flat lines without any endothermic peak and therefore, they are not shown here. Curve A shows an endothermic peak ca. 68°C. The same result was reported in our previous article.[12] Note that TPU(PTMG)/PEO (curve C) has the same endothermic peak, revealing that the addition of TPU(PTMG) into PEO does not change the T_m of PEO, and that TPU(PTMG) and PEO are immiscible and this blend is phase separated. On curve B, 66°C for T_m of TPU(PEG)/PEO was found rather than 68°C for PEO. This shift of T_m for PEO is due to permeation of TPU(PEG)

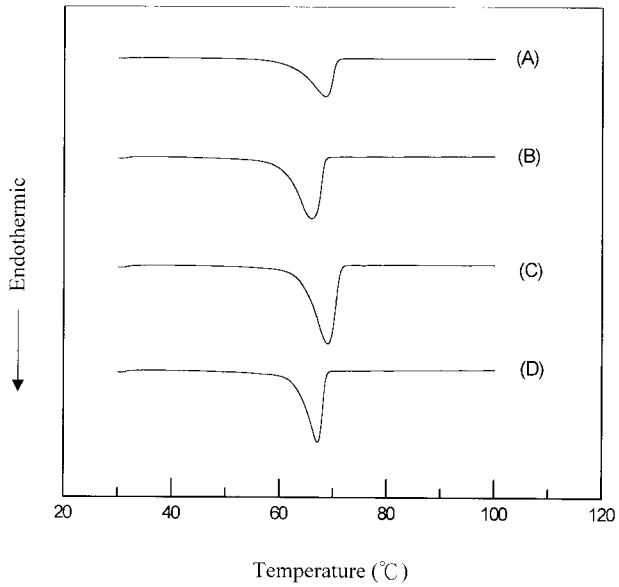

Figure 8 DSC thermograms of TPU blends. (A) PEO, (B) TPU(PEG)/PEO 50/50, (C) TPU(PTMG)/PEO 50/50, (D) TPU(PEG)/TPU(PTMG)/PEO 33/33/33.

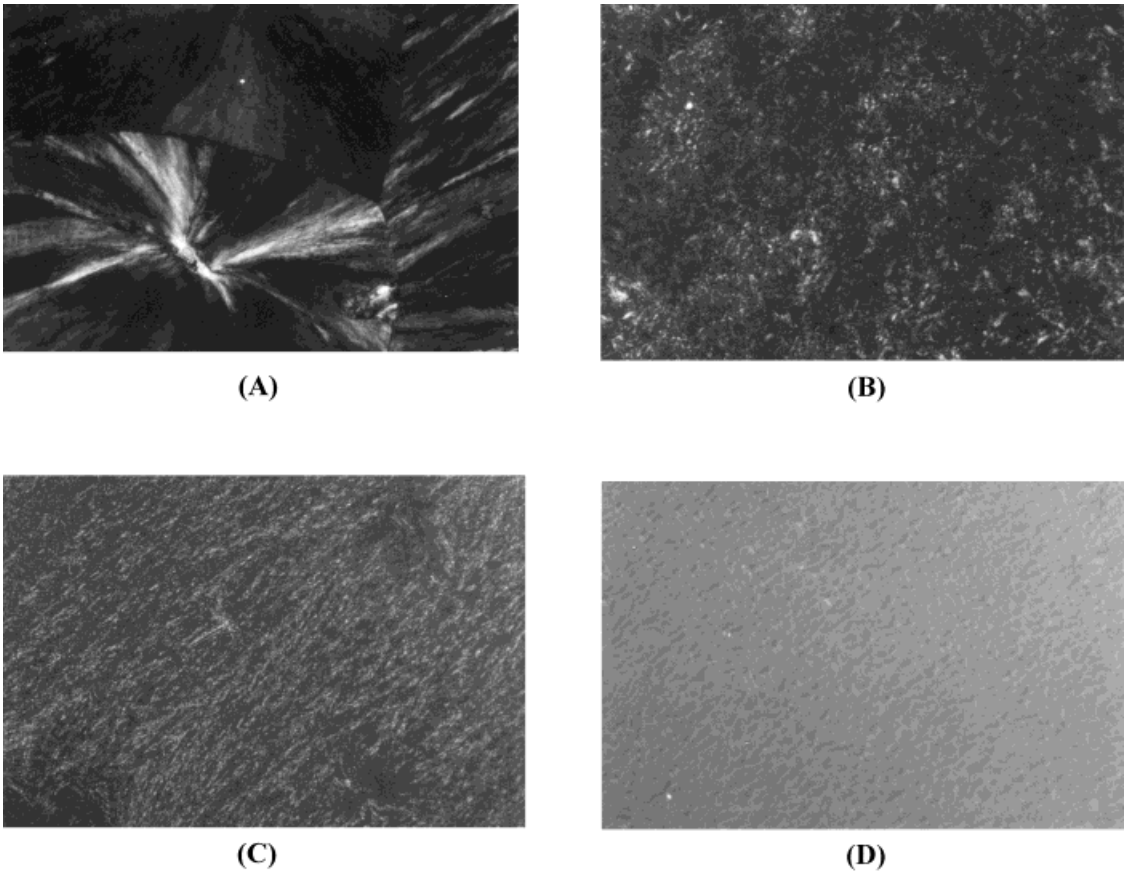

Figure 9 The enlarged (×200) photographs of PM for TPU(PEG)/PEO blends. TPU-(PEG)/PEO: (A) 15/85, (B) 29/71, (C) 58/42, and (D) 100/0.

into PEO spherulites, rendering TPU(PEG) and PEO partially miscible. With the addition of TPU(PEG) in TPU(PTMG)-PEO binary (curve D), the T_m peak moves to 67°C, evidence that TPU(PEG) plays a role as miscibility promoter between TPU(PTMG) and PEO. The thermograms were also used to determine the degree of crystallinity. This was done by integrating and obtaining the normalized area under the endothermic peaks. Based on these results also the above conclusions could be seen with the alternation in crystallinity and misciblity.

PM Results

According to the above discussion, the dry composite with the compositions shown in Table I should possess various morphologies due to various compatibility and/or miscibility of the polymer compositions. Thus, PM graphs were taken to clarify the speculation. All TPU(PEG)/PEO and TPU(PEG)/TPU(PTMG)/PEO were transparent just above the melting point of PEO. Optical micrographs of TPU(PEG)/PEO are shown in Figure 9. Because the PEO spherulites fill the volume completely and there is no evidence that the amorphous component segregates in large domains in interspherulitic contact areas, we concluded that TPU(PEG) and uncrystallized PEO are trapped between the crystalline lamellae of PEO. Figure 9(A) shows that crystalline PEO consists of radial spherulites with a clear boundary. On Figure 9(D), the polarizing photograph of TPU(PEG) displays the dark image for the amorphous morphology. In 29/71 TPU(PEG)/PEO, the PEO crystalline boundary disappears completely and a large number of small crystallites are dispersed in the volume [Fig. 9(B)]. Thus, TPU(PEG) is demonstrated to be partially miscible with PEO. With the increase in TPU(PEG), the crystalline image decreases and the amorphous image increases uniformly.

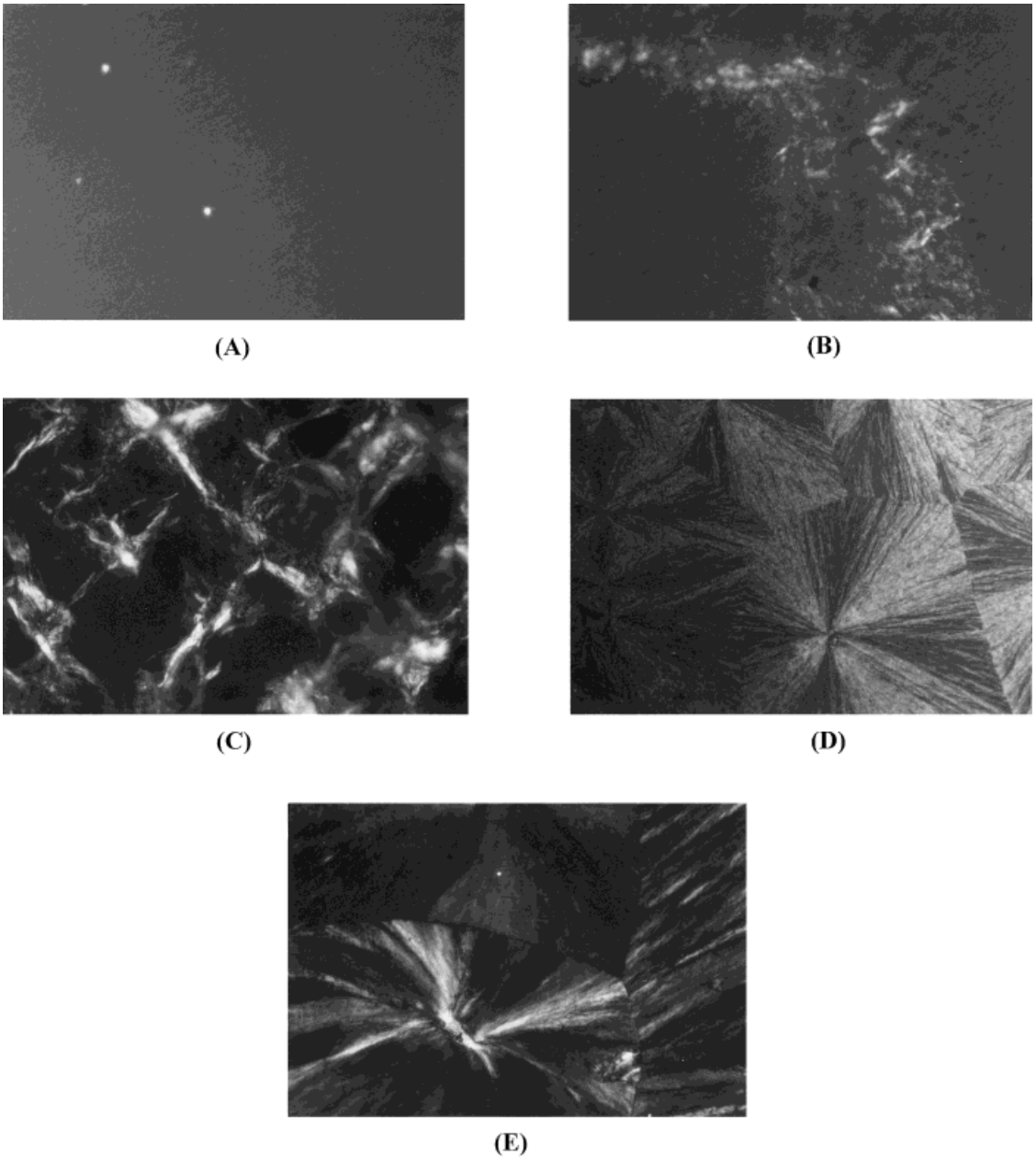

Figure 10 The enlarged (×200) photographs of PM for TPU(PEG)/TPU(PTMG)/PEO blends. TPU(PEG)/TPU(PTMG)/PEO: (A) 15/85/0, (B) 15/64/21, (C) 15/43/43, (D) 15/21/64, and (E) 15/0/85.

Figure 10 shows PM results for TPU(PEG)/TPU(PTMG)/PEO. Fifteen percent TPU(PEG) is used as an interfacial promoter for the composites to improve the miscibility. With high PEO content, the crystallinity is high and the spherulite boundary is obvious [Fig. 10(D and E)]. In 15/43/43 TPU(PEG)/TPU(PTMG)/PEO, the PEO crystalline boundary disappears and the shape is irregular [Fig. 10(C)]. Since the PEO spherulites growing in TPU(PEG)/TPU(PTMG)/PEO engulf the TPU(PEG), TPU(PTMG) and uncrystallized PEO, the radial orientation of lamellae with spherulites is disturbed by the presence of amorphous inclusions which constitute some spatial obstacles for spherulite growth. With increasing TPU(PTMG) content, the disturbance of radial orientation of lamellae becomes heavier, rendering the shape of PEO spherulites more irregular.

CONCLUSION

Using mixture design strategy, S_w and σ_{25} in the full compositional range of TPU(PEG)-TPU-(PTMG)-PEO are successfully modeled with a limited number of experiments. The coefficients of the regression models represented as contour plots, are extremely useful in studying the effects of polymer composition on S_w and σ_{25}. In conclusion, TPU(PTMG) provides the mechanical strength, PEO acts as the absorbent of $LiClO_4$-PC, and TPU(PEG) plays the role as compatibility promoter between TPU(PTMG) and PEO. Accordingly, the addition of TPU(PEG) in TPU(PTMG)-PEO binary blend provides the robust characteristics for the composite electrolyte and consequently the maximum S_w and σ_{25} can be obtained at the X_3 point [85% PEO, 15% TPU(PEG)]. The trade-off of the proper composite electrolytes, thus, is between a high conductivity and a strong mechanical property.

The financial support of this work by the National Science Council of the Republic of China under contract NSC 89-2214-E-006-012, is gratefully acknowledged. The authors highly appreciate Dr. A. Gopalan for his profound contribution to this revised manuscript.

REFERENCES

1. Sotele, J. J.; Soldi, V.; Nunes Pires, A. T. Polymer 1997, 38, 1179–1185.
2. Zheng, H.; Zheng, S.; Guo, Q.; J Polym Sci Part A Polym Chem 1997, 35, 3169–3179.
3. Yen, M. S.; Kuo, S. C. J Appl Polym Sci 1998, 67, 1301–1311.
4. Wright, P.V. Brit Polym J 1975, 7, 319.
5. Armand, M.; Chabagno, J. M.; Duclot, M. Fast Ion Transport in Solid; Vashishta, P., Ed.; North-Holland: New York, 1979; p. 131.
6. Wen, T. C.; Wang, Y. J.; Cheng, T. T.; Yang, C. H. Polymer 1999, 40, 3979–3988.
7. Ichino, T.; Matsumoto, M. J Polym Sci Part A Polym Chem 1993, 31, 589–591.
8. Ichino, T.; Matsumoto, M.; Rutt, J. S.; Nishi, S. J Polym Sci Part A Polym Chem 1993, 31, 1701–1707.
9. Rutt, J. S.; Matsumoto, M.; Ichino, T.; Nishi, S.; J Polym Sci Part A Polym Chem 1994, 32, 779–787.
10. Matsumoto, M.; Ichino, T.; Rutt, J. S.; Nishi, S. J Polym Sci Part A Polym Chem 1994, 32, 2551–2558.
11. Matsumoto, M.; Ichino, T.; Nishi, S.; J Electrochem Soc 1994, 141, 1989–1993.
12. Matsumoto, M. Polymer 1996, 37, 625–631.
13. Wen, T. C.; Chang, J. S.; Cheng, T. T. J Electrochem Soc 1998, 145, 3450–3455.
14. Cheng, T. T.; Wen, T. C. J Electroanal Chem 1998, 459, 99–110.
15. Cheng, T. T.; Wen, T. C. Solid State Ionics 1998, 107, 161–171.
16. Yang, C. H.; Li, Y. J.; Wen, T. C. Ind Eng Chem Res 1997, 36, 1614–1621.
17. Lin, S. M.; Wen, T. C. J Appl Electrochem 1993, 23, 487–494.
18. Yang, C. H.; Yang, H. J.; Wen, T. C.; Wu, M. S.; Chang, J. S. Polymer 1999, 40, 871–885.
19. Odian, G. Principles of Polymerization, 3rd ed.; Wiley-Interscience: New York, 1991; Chapter 1.
20. Cornell, J. A. Experiments with Mixtures: Design, Models and the Analysis of Mixture Data, 2nd ed.; John Wiley & Sons: New York, 1990.